



Optical emission from single, charge-tunable quantum rings

R.J. Warburton^{a,*}, C. Schäfflein^a, D. Haft^a, F. Bickel^a, A. Lorke^a, K. Karrai^a, J.M. Garcia^b,
W. Schoenfeld^b, P.M. Petroff^b

^aCenter for NanoScience and Sektion Physik, Ludwig-Maximilians-Universität, Geschwister-Scholl-Platz 1, 80539 München, Germany

^bMaterials Department and QUEST, University of California, Santa Barbara, CA 93106, USA

Abstract

We have succeeded in preparing excitons with a specific charge in single semiconductor quantum rings. Buried InAs quantum rings are loaded with electrons from a reservoir through a tunneling barrier and an additional electron–hole pair is generated by optical excitation. Single rings are addressed with nano-optical techniques. We observe abrupt shifts in the emission energy as electrons are added one by one. Furthermore, the experiments provide unique insights into the interaction of electrons in semiconductor nano-islands with their environment. © 2001 Elsevier Science B.V. All rights reserved.

Keywords: Quantum dots; Photoluminescence; Tunneling

1. Introduction

Semiconductor quantum dots confine electrons and holes in all three directions and have therefore atomic-like properties. For instance, when a quantum dot is filled sequentially with electrons, the charging energies are pronounced for particular electron numbers [1,2], exactly as in atomic physics where the shell filling is described by Hund's rules. Semiconductor quantum dots have also a valence band with strong optical transitions to the conduction band. These interband transitions form the basis for much

of the interest in the optical properties of quantum dots [3], and in their application as the gain medium in lasers [3], as storage elements [4–7], and as fluorescent optical markers [8]. The issue we address here is how the interband transitions of a *single* quantum dot change as electrons are added *one by one*.

Our motivation is two-fold. First, the shifts in emission energies on charging, and also the appearance of satellites for highly charged dots, are direct measures of the Coulomb interactions between the particles. This is a model system for the investigation of Coulomb correlations because we have a known small number of confined particles. Secondly, by weakly coupling a dot to a reservoir of charge, we can explore the interactions between the electrons in the quantum dot and their environment. In particular, we show here how we can use the optical emission of

* Correspondence address: Department of Physics, Heriot-Watt University, Edinburgh EH14 4AS, UK. Tel.: +44-131-4518069; fax: +44-131-4513136.

E-mail address: r.j.warburton@hw.ac.uk (R.J. Warburton).

a quantum dot as a probe of the tunneling of electrons into the dot. Also, for highly charged dots, we show how we can use the line width of the emission as a measure of the energy relaxation rate.

2. Sample design and experiments

The quantum dots were grown by depositing InAs on GaAs in the Stanski–Krastanow mode followed by the overgrowth of GaAs [9]. With continuous overgrowth, the dots emit at 1.1 eV and can accommodate up to six electrons [2,10,11]. Unfortunately, there are no commercially available detectors capable of photon counting at 1.1 eV and this makes single-dot spectroscopy formidably difficult. We have concentrated instead on quantum rings. The rings are grown like the dots, but a growth pause is introduced after the dots have been partially overgrown with GaAs. The mobile indium diffuses laterally to such an extent that the dots become ring-like [12,13]. Overall, the rings are thinner in the growth direction than the dots and this increases the band gap to 1.3 eV where we can detect the emission with a Si CCD camera. However, the rings can accommodate fewer electrons than the dots before the charge spills out into the wetting layer, the thin InAs layer connecting all the rings. In our analysis of the optical emission, we assume an s-like ground state and a p-like excited state. Note that this holds equally for dots and rings so that the general features of shell filling and satellite emission are expected to be the same for both dots and rings. The absolute energy shifts on charging will depend however on the exact form of the confining potential. Aharonov–Bohm effects in the rings are not relevant here as we do not apply a magnetic field.

In order to populate quantum rings with electrons, we use a charge-tunable device, as shown in Fig. 1. The rings are situated 25 nm from an n^+ -region, a reservoir of electrons, and 150 nm from a Schottky gate on the sample surface. We apply a voltage between the gate and n^+ -region. At large, negative gate voltages (V_g^1 in Fig. 1b), the ring level lies well above the Fermi energy and is unoccupied. At a more positive V_g , the ring level is resonant with the Fermi energy and electrons tunnel into and out of the rings. A further increase in V_g (V_g^2 in Fig. 1b) traps one electron in the ring. We can monitor the tunneling

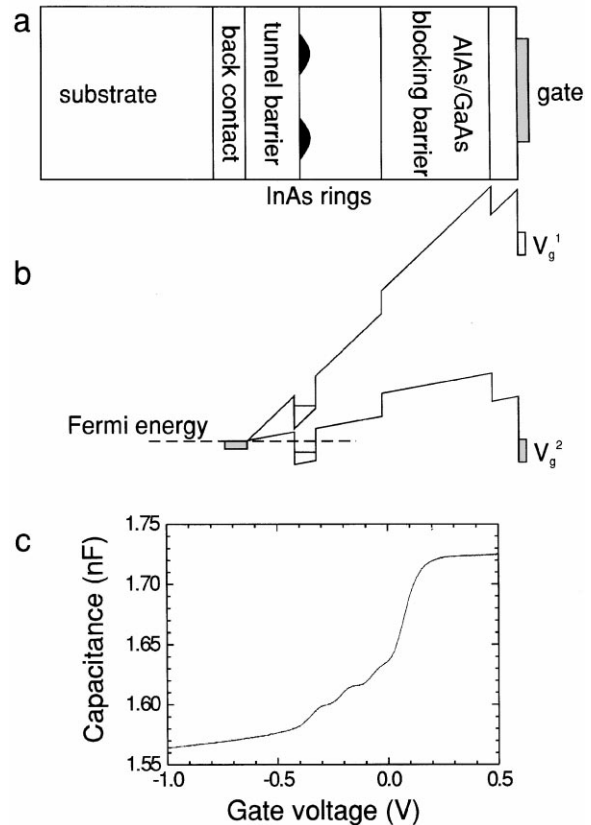


Fig. 1. (a) The layer structure of our device. The tunnel barrier is 25 nm thick, and the separation between back contact and surface is 175 nm. (b) The band diagram at two different voltages, V_g^1 and V_g^2 . (c) The capacitance of the device used for the optical experiments (gate area 1.8 mm²) at 4.2 K.

with the capacitance between gate and back contact [14]. Fig. 1c shows the capacitance of the device used for the optical experiments. There are three charging peaks, inevitably inhomogeneously broadened in this large-area device. The rise in the signal at $V_g = 0.1$ V corresponds to tunneling into the wetting layer.

The inhomogeneous broadening in the interband spectra of the rings is remarkably small, just 18 meV for the fundamental transition. However, this broadening is still larger than the binding energies of charged excitons and biexcitons, typically a few meV. It is therefore necessary to measure a single ring rather than an ensemble. We have measured the photoluminescence (PL) at low temperature with a confocal microscope which has a diffraction-limited spatial resolution

of 610 nm at a wavelength of 900 nm. Our ring densities are $\sim 5 \times 10^9 \text{ cm}^{-2}$ implying that tens of rings lie in the focus. However, by a further discrimination in wavelength, we could always isolate individual rings which emit in the low-energy tail of the distribution. We have also investigated rings closer to the center of the ensemble distribution by increasing the spatial resolution with 300 nm apertures in an aluminum film on the sample surface. In both cases, even when several rings are detected simultaneously, PL peaks can be associated with particular rings with a good degree of certainty by examining the V_g dependence.

We excited PL in the dots by pumping the wetting layer with a laser diode emitting at 822 nm. Excitons relax into the rings from the continuum in the wetting layer. We made sure that we have not more than one exciton in a ring at any moment in time by keeping the power below a limit which we estimated by making the most optimistic assumptions on the throughput of our optics and on the capture efficiency and quantum efficiency of our sample. For the unmasked samples, this limit is $\sim 1 \mu\text{W}$. Reassuringly, at large, negative V_g , we observe only a single PL line from each ring, i.e. there is no indication of the fine structure which emerges when a dot is occupied by several excitons [15,16]. The PL was dispersed with a 0.25 m grating spectrometer and detected with a cooled CCD camera, a setup with spectral resolution 0.2 nm .¹ This corresponds to an energy resolution of 0.3 meV at the typical emission energy of 1.3 eV . This is not sufficient to resolve many of the lines. The homogeneous line widths may be in the μeV regime and it is an outstanding challenge to measure them.

3. Shell-filling

Fig. 2 is a grey-scale plot of the PL as a function of V_g . At $V_g \sim -0.7 \text{ V}$ there is a single, sharp peak which is the emission from a single ring. As V_g increases, Fig. 2 shows that the PL wavelength increases step-wise and four steps can be made out. These steps all occur when an additional electron becomes trapped in the ring. The first step at -0.6 V marks the transition

¹The (imaging) spectrometer has an asymmetric response in wavelength and this instrumental effect is responsible for the high-energy tail in the unresolved peaks of Fig. 4.

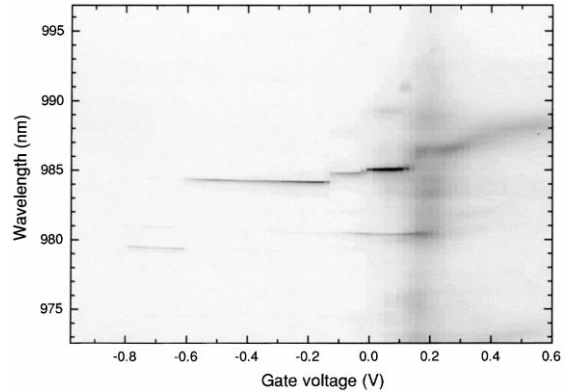


Fig. 2. A grey-scale plot of the photoluminescence (PL) vs gate voltage at 4.2 K. The PL intensity is related linearly to the degree of darkness.

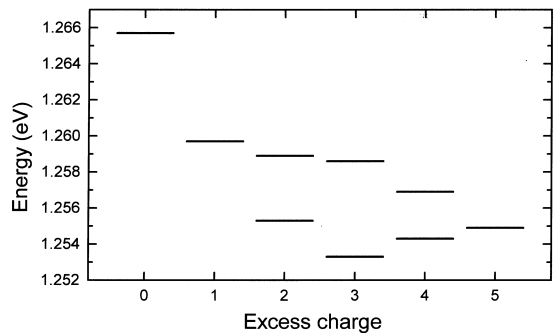


Fig. 3. PL emission energy against additional charge measured on a single quantum ring.

from emission from a neutral exciton X , to emission from a singly charged exciton, X^{1-} . The shift is to the red, i.e. the energy decreases. The decrease, 6.0 meV , corresponds to the binding energy of the X^{1-} . The second jump represents the transition from X^{1-} to X^{2-} , and so on.

It is clear in Fig. 2 that the jumps in energy are not all equal. The first is large, the second small, the third also small, yet the fourth and fifth are reasonably large, as shown explicitly in Fig. 3, a plot of emission energy against charge. The large shift from X to X^{1-} , which is larger incidentally than the 4 meV shift of our InAs dots [10], can be thought of in a simple picture as a consequence of the hole wave function being more localized than the electron wave function. On going from X to X^{1-} , the repulsion between the two

electrons is more than compensated by the attraction between the additional electron and hole. The shifts of the more highly charged excitons represent an optical manifestation of shell-filling [17]. The main difference in the transitions arises through the exchange interaction. For X^{1-} and X^{2-} , the s electron which recombines with the hole has no exchange interaction with the p electrons. The shifts in the transitions from X^{1-} to X^{2-} and X^{2-} to X^{3-} are therefore small and similar. Conversely, for X^{4-} , one of the p electrons is forced to have the same spin as the electron which recombines, and hence there is an exchange interaction between this s electron and the p electrons in the initial state. This interaction reduces the PL energy, giving a large shift between X^{3-} and X^{4-} . A similar argument holds also for X^{5-} . In this way, large shifts arise whenever a sub-level is completely filled in the initial state.

4. Satellites

For highly charged excitons, X^{2-} and above, a satellite appears on the long wavelength (low energy) side of the main peak. The satellites can be just made out in the grey-scale plot (Fig. 2), but are obvious features in the spectra plotted in Fig. 4 [17]. Although we never measure only a single ring, there are two reasons why we can be sure that the satellites and main peaks come from the same ring. Firstly, the X^{2-} satellite appears exactly at the V_g where the transition from X^{1-} to X^{2-} takes place. Similarly, both the main peak and satellite move together in the transition from X^{2-} to X^{3-} . It is highly unlikely that two different rings would exhibit transitions at exactly the same V_g . Secondly, in the transition from X^{1-} to X^{2-} , the main peak decreases in intensity although there is a global trend of increasing intensity with increasing V_g . The lost intensity of the main peak is taken up by the satellite such that the overall intensity stays constant to within 10%. This supports strongly our assertion that the main and satellite PL arise from the same ring.

We argue that the ring has two emission energies for the X^{2-} because there are two different final states. This is illustrated in the icons of Fig. 4, where we plot the level structure, labelling the states with angular momentum quantum number, 0 for the s level, ± 1 for the p level. For X^{2-} , the two electrons left

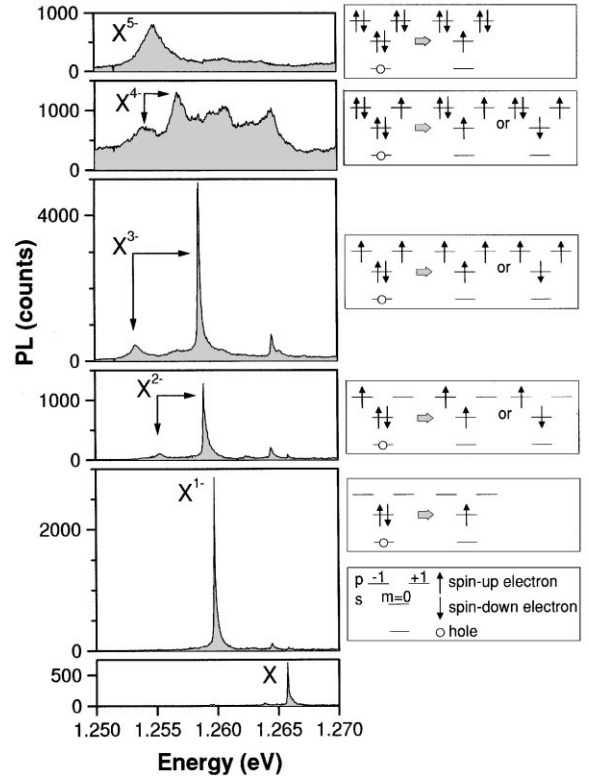


Fig. 4. PL spectra at $V_g = -0.76, -0.16, -0.10, 0.40, 0.22$ and 0.50 V, corresponding to emission from the X, X^{1-} , X^{2-} , X^{3-} , X^{4-} , and X^{5-} excitons, respectively. The PL red-shifts on charging and a satellite occurs on the low-energy side of the main peak for X^{2-} and X^{3-} . Note that the other, weaker emissions (for instance on the high-energy side of the main X^{2-} PL) belong in all probability to other rings. The broad peak between the X^{3-} main peak and satellite may be emission from an excited initial state which recombines before it can relax. The level diagrams show the emission processes from initial state to possible final states. We consider s and p states in the conduction band with angular momentum 0, ± 1 , and the s state in the valence band. In the experiment, both electrons and holes are unpolarized. To avoid redundancy, we sketch cases with electrons preferentially polarized up and an unpolarized hole.

over after the photon has been emitted can have parallel spin and therefore an energy reduced by the exchange interaction. A low-energy final state implies a large PL energy. Therefore, we associate the main peak with the spin-parallel final state. Alternatively, the two electrons in the final state can have antiparallel spins, giving rise to a higher final state energy and hence a lower PL energy. The satellite emission corresponds then to the spin-antiparallel final state.

The states sketched in Fig. 4 assume an initial spin polarization but spins are equally likely up as down in the present experiment. The spin-parallel final state is therefore a triplet with Coulomb energy $E_{\text{sp}}^{\text{c}} - E_{\text{sp}}^{\text{x}}$ where E_{sp}^{c} (E_{sp}^{x}) is the direct (exchange) interaction between an s and a p electron. The spin-antiparallel state is a singlet with energy $E_{\text{sp}}^{\text{c}} + E_{\text{sp}}^{\text{x}}$. This is in exact analogy to the excited states of the helium atom. The splitting between main and satellite PL is therefore twice the exchange energy, implying that $E_{\text{sp}}^{\text{x}} = 1.8$ meV for this particular ring. From the degeneracies, we expect the main peak to be three times stronger than the main peak. By comparing the area under the two peaks, we find that the intensity ratio is $7 \pm 2 : 1$, not the $3 : 1$ expected from the degeneracies alone. A possible explanation for the suppression of the satellite is the electron-hole exchange interaction which tends to align electron and hole spins in the initial state [18,19], favoring emission into the triplet final state.

For the X^{3-} , the separation between the main PL and satellite is increased (Figs. 3 and 4). For the X^{3-} there are two final states which can be reached through optical emission. They are analogous to the excited states of the Li atom, and can be found by diagonalizing the interaction Hamiltonian for three spin- $\frac{1}{2}$ electrons (see, for example, Ref. [20]). In this model, we calculate a splitting of $3E_{\text{sp}}^{\text{x}}$ and an intensity ratio $2 : 1$. This agrees remarkably well with the experimental results. We find for X^{3-} that the splitting between the satellite and main peak is 1.44 times that for X^{2-} , very close to the predicted 1.5. Furthermore, on going from X^{2-} to X^{3-} , the satellite does become more intense relative to the main peak. For X^{3-} , the main PL is 2 ± 0.5 times stronger than the satellite.

Decay of the X^{3-} is the most complicated case. X^{4-} is one electron short of a filled p shell and therefore should behave exactly like X^{2-} which has a single p electron. We expect therefore that the splitting between satellite and main peak for X^{4-} is also $2E_{\text{sp}}^{\text{x}}$, as for X^{2-} . Experimentally, the splitting for X^{4-} does return to approximately the value for X^{2-} , but the PL becomes very broad making a more detailed analysis difficult.

By making the analogy to the helium atom, we are essentially treating the Coulomb interaction as a perturbation to the single-particle structure. In terms of lengths, the assumption is valid when the electron and hole wave functions extend less than the

excitonic Bohr radius (10 nm). This is certainly not the case along the circumference of the ring which is ca. 100 nm. It is perhaps surprising that perturbation theory can predict the relative shifts so well. We comment, however, that perturbation theory using harmonic oscillator wave functions for the electrons and holes [21] reproduces qualitatively the features in the PL on charging, but it does not account quantitatively for all the energetic shifts. For the rings, we require either drastically different single-particle states and/or a more complete treatment of the Coulomb interactions.

5. Relaxation

An obvious feature in the spectra of Fig. 4 is that the satellite peaks are broader than the main peaks. For the X^{2-} for instance, the satellite has a FWHM of 0.6 meV, clearly larger than the unresolved main peak with $\text{FWHM} < 0.25$ meV (see footnote 1). Our explanation is that the widths reflect different relaxation rates. For highly charged excitons, X^{2-} and above, the final state after emission of a photon is an excited state. There is a vacancy in the s shell yet occupation of the p shell. In the simplest case, the ring emits a photon and then some time later the final state relaxes into its ground state. If the final state relaxes very quickly however, the emission is broadened by an energetic fuzziness of the final state. In other words, the PL line width reflects the relaxation rate.

To explain why the two PL peaks have different widths, and therefore different relaxation rates, we consider the X^{2-} . The main difference between the two possible final states is the spin: after emission into the main peak, the final state is a triplet with total spin $S = 1$; after emission into the satellite, the final state is a singlet with $S = 0$. The different spins influence the relaxation rates into the $S = 0$ ground state: for the triplet, relaxation requires a spin-flip; for the singlet, it does not. Relaxation proceeds either through phonon emission or through Auger-like processes with another electron, most likely in the wetting layer. Phonon emission obviously conserves spin; Auger preferentially swaps the spins of the two participating electrons [22]. We are thus led to the following conclusions: for emission into the singlet final state (satellite PL), relaxation takes place by phonon

emission, and is fast on the timescale of recombination. Directly from the line width, we infer a decay time of 1.1 ps. There is therefore no phonon bottleneck. For emission into the triplet final state (main PL), phonon emission is no longer possible, and the relaxation is noticeably slower.

The same argument also holds for the X^{3-} : the satellite is broad (FWHM 1.2 meV) because relaxation can take place without a spin-flip; the main peak is narrower because relaxation requires a spin-flip.

An obvious feature in Figs. 2 and 4 is the enormous broadening and increase in intensity in the PL at $V_g \sim 0.1$ V. We know from the capacitance that the wetting layer becomes occupied at this voltage which strongly suggests that interactions between electrons in the ring and electrons in the wetting layer are important. The broadening in the PL can therefore arise from the many possible initial state energies once the continuum in the wetting layer is occupied [15]. At higher voltages, above 0.1 V, the PL does settle into a peak once more, but with a large width. We propose that with a large population in the continuum, the final state can always relax quickly through strong Auger processes, independent of spin, and this broadens the PL. The increase in PL intensity is partly caused by an increase in capture efficiency, but it is hard to say if this is the only factor.

6. Tunneling

At large and negative V_g , the PL disappears which we interpret as field ionization of the excitons [23]. The electron tunnels out of the ring before recombination can take place. At larger V_g , the 0- and 1-electron states become degenerate and electrons tunnel into and out of the ring. We can monitor the tunneling optically because the X and X^{1-} excitons have different energies. Fig. 5 shows the PL in the transition regime from X to X^{1-} , and also X^{1-} to X^{2-} . In both cases, it can be seen how the high-energy peak weakens and the low-energy peak strengthens without any detectable emission in between.

It is surprising that we observe two PL lines over a large range of gate voltage. The most obvious explanation is that there are temporal fluctuations in the ring's potential giving rise to fluctuations in the ring's charge. The potential fluctuations must be large how-

ever because we see both PL peaks over a 20 mV range of V_g , corresponding to 3 meV in potential energy. This energy scale rules out thermal fluctuations and also ring–ring interactions as explanations for the fluctuations as their characteristic energy scales are too small, 0.4 and 1 meV, respectively [14]. The only remaining possibility is that the fluctuations are caused by random occupation of an impurity state close to the ring. We note that this is not the first observation of fluctuations in quantum dots: they have been invoked to account for broad single-electron tunneling peaks [24] and also spectral diffusion in PL [25]. They clearly warrant further investigation, particularly given the current interest in coherent manipulation of the states in quantum dots [26].

7. Conclusions

We list the main points emerging from these experiments on single, charge-tunable quantum rings. Firstly, we have observed Coulomb blockade by monitoring the emission energy of a single ring. Whenever a ring gains an additional electron, the emission shifts to the red. Whenever the charge in the ring stays constant, the emission exhibits only a very small Stark shift. Secondly, the sizes of the jumps in the emission energy exhibit shell effects: the jump is large whenever a shell is completely filled in the initial state. Thirdly, we have observed satellite emissions for highly charged excitons which arise through nondegenerate final states. Fourthly, the line widths of the satellite emission are larger than those of the main emission, which can be accounted for by spin-dependent relaxation. In particular, we can distinguish between Auger and phonon scattering: relaxation through phonon emission occurs on a ps-timescale; Auger processes are comparably fast only when there is a sizable electron population in the wetting layer. Finally, by investigating the tunneling regimes, we are forced to invoke temporal fluctuations in the ring's potential.

Acknowledgements

We would like to thank J.P. Kotthaus for stimulating discussions. This work was funded by the DFG

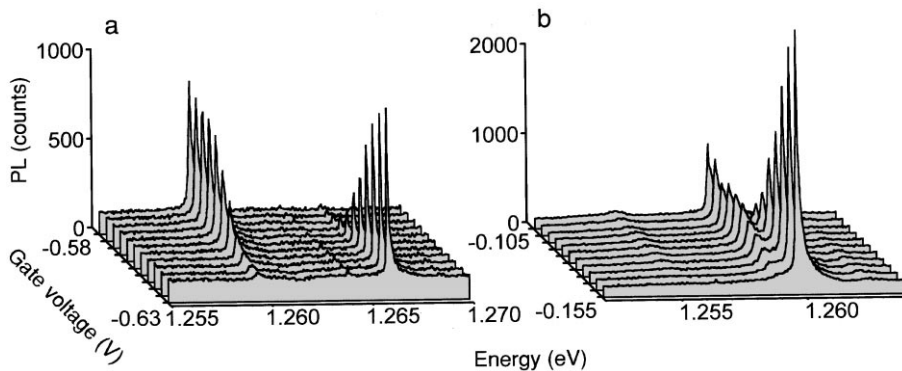


Fig. 5. PL spectra in the transition region from X to X^{1-} (a) and from X^{1-} to X^{2-} (b). b shows also the emergence of the satellite at 1.255 eV.

(Project SFB 348) and by QUEST, a NSF Science and Technology Center.

References

- [1] S. Tarucha, D.G. Austing, T. Honda, R.J. van der Hage, L.P. Kouwenhoven, *Phys. Rev. Lett.* **77** (1996) 3613.
- [2] B.T. Miller et al., *Phys. Rev. B* **56** (1997) 6764.
- [3] D. Bimberg, M. Grundmann, N.N. Ledentsov, *Quantum Dot Heterostructures*, Wiley, Chichester, 1998.
- [4] G. Yusa, H. Sakaki, *Appl. Phys. Lett.* **70** (1997) 345.
- [5] J.J. Finley et al., *Appl. Phys. Lett.* **73** (1998) 2618.
- [6] M.C. Bödefeld, R.J. Warburton, K. Karrai, J.P. Kotthaus, G. Medeiros-Ribeiro, P.M. Petroff, *Appl. Phys. Lett.* **74** (1999) 1839.
- [7] T. Lundström et al., *Science* **286** (1999) 2312.
- [8] M. Bruchez Jr., M. Moronne, P. Gin, S. Weiss, A.P. Alivisatos, *Science* **281** (1998) 2013.
- [9] D. Leonard, K. Pond, P.M. Petroff, *Phys. Rev. B* **50** (1994) 11 687.
- [10] R.J. Warburton, C.S. Dürr, K. Karrai, J.P. Kotthaus, G. Medeiros-Ribeiro, P.M. Petroff, *Phys. Rev. Lett.* **79** (1997) 5282.
- [11] H. Drexler, D. Leonard, W. Hansen, J.P. Kotthaus, P.M. Petroff, *Phys. Rev. Lett.* **73** (1994) 2252.
- [12] J.M. Garcia et al., *Appl. Phys. Lett.* **71** (1997) 2014.
- [13] A. Lorke et al., *Phys. Rev. Lett.* **84** (2000) 2223.
- [14] G. Medeiros-Ribeiro, F.G. Pikus, P.M. Petroff, A.L. Efros, *Phys. Rev. B* **55** (1997) 1568.
- [15] E. Deckel et al., *Phys. Rev. Lett.* **80** (1998) 4991.
- [16] L. Landin, M.S. Miller, M.-E. Pistol, C.E. Pryor, L. Samuelson, *Science* **280** (1998) 262.
- [17] A. Wojs, P. Hawrylak, *Phys. Rev. B* **55** (1997) 13 066.
- [18] E. Blackwood, M.J. Snelling, R.T. Harley, S.R. Andrews, C.T.B. Foxon, *Phys. Rev. B* **50** (1994) 14 246.
- [19] M. Bayer et al., *Phys. Rev. Lett.* **82** (1999) 1748.
- [20] L.I. Schiff, *Quantum Mechanics*, Third Edition, McGraw-Hill, 1968, p. 377.
- [21] R.J. Warburton et al., *Phys. Rev. B* **58** (1998) 16 221.
- [22] B.K. Ridley, *Quantum Processes in Semiconductors*, Clarendon Press, Oxford, 1982.
- [23] K.H. Schmidt, G. Medeiros-Ribeiro, P.M. Petroff, *Phys. Rev. B* **58** (1998) 3597.
- [24] B.T. Miller et al., *Physica B* **249–251** (1998) 257.
- [25] S.A. Empedocles, M.G. Bawendi, *Science* **278** (1997) 2114.
- [26] N.H. Bonadeo, J. Erland, D. Gammon, D. Park, D.S. Katzer, D.G. Steel, *Science* **282** (1998) 1473.